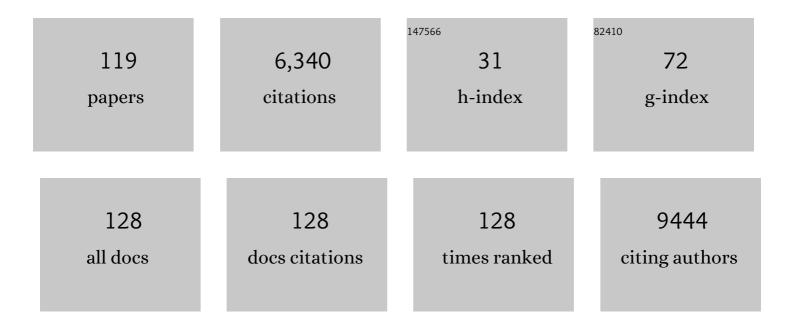
## Kristoffer Hougaard Madsen

List of Publications by Year in descending order

Source: https://exaly.com/author-pdf/1728139/publications.pdf Version: 2024-02-01



#	Article	IF	CITATIONS
1	Toward discovery science of human brain function. Proceedings of the National Academy of Sciences of the United States of America, 2010, 107, 4734-4739.	3.3	2,703
2	Non-white noise in fMRI: Does modelling have an impact?. NeuroImage, 2006, 29, 54-66.	2.1	370
3	Automatic skull segmentation from MR images for realistic volume conductor models of the head: Assessment of the state-of-the-art. NeuroImage, 2018, 174, 587-598.	2.1	198
4	Neural correlates of virtual route recognition in congenital blindness. Proceedings of the National Academy of Sciences of the United States of America, 2010, 107, 12716-12721.	3.3	160
5	Are Movement Artifacts in Magnetic Resonance Imaging a Real Problem?—A Narrative Review. Frontiers in Neurology, 2017, 8, 232.	1.1	129
6	Model sparsity and brain pattern interpretation of classification models in neuroimaging. Pattern Recognition, 2012, 45, 2085-2100.	5.1	115
7	SimNIBS 2.1: A Comprehensive Pipeline for Individualized Electric Field Modelling for Transcranial Brain Stimulation. , 2019, , 3-25.		115
8	Deep convolutional neural networks for interpretable analysis of EEG sleep stage scoring. , 2017, , .		107
9	A principled approach to conductivity uncertainty analysis in electric field calculations. NeuroImage, 2019, 188, 821-834.	2.1	96
10	Electric field simulations for transcranial brain stimulation using FEM: an efficient implementation and error analysis. Journal of Neural Engineering, 2019, 16, 066032.	1.8	95
11	How to target inter-regional phase synchronization with dual-site Transcranial Alternating Current Stimulation. Neurolmage, 2017, 163, 68-80.	2.1	94
12	Recovery from optic neuritis: an ROI-based analysis of LGN and visual cortical areas. Brain, 2007, 130, 1244-1253.	3.7	83
13	Shift-invariant multilinear decomposition of neuroimaging data. NeuroImage, 2008, 42, 1439-1450.	2.1	81
14	Accurate and robust whole-head segmentation from magnetic resonance images for individualized head modeling. NeuroImage, 2020, 219, 117044.	2.1	73
15	No trace of phase: Corticomotor excitability is not tuned by phase of pericentral mu-rhythm. Brain Stimulation, 2019, 12, 1261-1270.	0.7	70
16	Accessibility of cortical regions to focal TES: Dependence on spatial position, safety, and practical constraints. NeuroImage, 2019, 203, 116183.	2.1	67
17	Motivational Tuning of Fronto-Subthalamic Connectivity Facilitates Control of Action Impulses. Journal of Neuroscience, 2014, 34, 3210-3217.	1.7	66
18	Simultaneous representation of a spectrum of dynamically changing value estimates during decision making. Nature Communications, 2017, 8, 1942.	5.8	66

#	Article	IF	CITATIONS
19	Abnormal dopaminergic modulation of striato-cortical networks underlies levodopa-induced dyskinesias in humans. Brain, 2015, 138, 1658-1666.	3.7	65
20	An fMRI study of the neural correlates of graded visual perception. NeuroImage, 2006, 31, 1711-1725.	2.1	63
21	The acute brain response to levodopa heralds dyskinesias in Parkinson disease. Annals of Neurology, 2014, 75, 829-836.	2.8	61
22	Concurrent TMS-fMRI for causal network perturbation and proof of target engagement. NeuroImage, 2021, 237, 118093.	2.1	56
23	Visualization of nonlinear kernel models in neuroimaging by sensitivity maps. NeuroImage, 2011, 55, 1120-1131.	2.1	55
24	<scp>R</scp> estingâ€state connectivity predicts levodopaâ€induced dyskinesias in <scp>P</scp> arkinson's disease. Movement Disorders, 2016, 31, 521-529.	2.2	53
25	Migraine with visual aura associated with thicker visual cortex. Brain, 2018, 141, 776-785.	3.7	52
26	Variation in the oxytocin receptor gene is associated with behavioral and neural correlates of empathic accuracy. Frontiers in Behavioral Neuroscience, 2014, 8, 423.	1.0	49
27	Working Memory Modulation of Frontoparietal Network Connectivity in First-Episode Schizophrenia. Cerebral Cortex, 2017, 27, 3832-3841.	1.6	49
28	Generalizability of machine learning for classification of schizophrenia based on restingâ€state functional MRI data. Human Brain Mapping, 2020, 41, 172-184.	1.9	44
29	Multiple sclerosis impairs regional functional connectivity in the cerebellum. NeuroImage: Clinical, 2014, 4, 130-138.	1.4	42
30	Expanded functional coupling of subcortical nuclei with the motor resting-state network in multiple sclerosis. Multiple Sclerosis Journal, 2013, 19, 559-566.	1.4	39
31	Value and limitations of intracranial recordings for validating electric field modeling for transcranial brain stimulation. NeuroImage, 2020, 208, 116431.	2.1	39
32	Attenuated neural response to gamble outcomes in drug-naive patients with Parkinson's disease. Brain, 2013, 136, 1192-1203.	3.7	38
33	Images of Illusory Motion in Primary Visual Cortex. Journal of Cognitive Neuroscience, 2006, 18, 1174-1180.	1.1	35
34	Resting-state connectivity of pre-motor cortex reflects disability in multiple sclerosis. Acta Neurologica Scandinavica, 2013, 128, n/a-n/a.	1.0	33
35	Role of emotional processing in depressive responses to sex-hormone manipulation: a pharmacological fMRI study. Translational Psychiatry, 2015, 5, e688-e688.	2.4	31
36	Aberrant neural signatures of decision-making: Pathological gamblers display cortico-striatal hypersensitivity to extreme gambles. NeuroImage, 2016, 128, 342-352.	2.1	30

#	Article	IF	CITATIONS
37	Quantifying functional connectivity in multi-subject fMRI data using component models. Human Brain Mapping, 2017, 38, 882-899.	1.9	30
38	Neural markers of negative symptom outcomes in distributed working memory brain activity of antipsychotic-naive schizophrenia patients. International Journal of Neuropsychopharmacology, 2013, 16, 1195-1204.	1.0	28
39	Locus Coeruleus Shows a Spatial Pattern of Structural Disintegration in Parkinson's Disease. Movement Disorders, 2022, 37, 479-489.	2.2	27
40	Tuning the Brake While Raising the Stake: Network Dynamics during Sequential Decision-Making. Journal of Neuroscience, 2016, 36, 5417-5426.	1.7	25
41	Nonlinear denoising and analysis of neuroimages with kernel principal component analysis and pre-image estimation. Neurolmage, 2012, 60, 1807-1818.	2.1	24
42	The Myelin Content of the Human Precentral Hand Knob Reflects Interindividual Differences in Manual Motor Control at the Physiological and Behavioral Level. Journal of Neuroscience, 2021, 41, 3163-3179.	1.7	24
43	Postoperative increase in grey matter volume in visual cortex after unilateral cataract surgery. Acta Ophthalmologica, 2013, 91, 58-65.	0.6	23
44	Does pericentral mu-rhythm "power―corticomotor excitability? – A matter of EEG perspective. Brain Stimulation, 2021, 14, 713-722.	0.7	21
45	A checklist for assessing the methodological quality of concurrent tES-fMRI studies (ContES) Tj ETQq1 1 0.784	814 rgBT	/Overlock 10 Th
46	Neural correlates of taste perception in congenital olfactory impairment. Neuropsychologia, 2014, 62, 297-305.	0.7	20
47	Approximate LO constrained non-negative matrix and tensor factorization. , 2008, , .		19
48	Perspectives on Machine Learning for Classification of Schizotypy Using fMRI Data. Schizophrenia Bulletin, 2018, 44, S480-S490.	2.3	19
49	Shifted Non-Negative Matrix Factorization. IEEE International Workshop on Machine Learning for Signal Processing, 2007, , .	0.0	18
50	Archetypal Analysis for Modeling Multisubject fMRI Data. IEEE Journal on Selected Topics in Signal Processing, 2016, 10, 1160-1171.	7.3	17
51	Non-parametric Bayesian graph models reveal community structure in resting state fMRI. NeuroImage, 2014, 100, 301-315.	2.1	15
52	Transcranial Magnetic Stimulation: An Automated Procedure toÂObtain Coil-specific Models for Field Calculations. Brain Stimulation, 2015, 8, 1205-1208.	0.7	15
53	Measuring motion-induced B <sub>0</sub> -fluctuations in the brain using field probes. Magnetic Resonance in Medicine, 2016, 75, 2020-2030.	1.9	15
54	Getting to grips with endoscopy - Learning endoscopic surgical skills induces bi-hemispheric plasticity of the grasping network. NeuroImage, 2019, 189, 32-44.	2.1	15

#	Article	IF	CITATIONS
55	Cortical neuroplasticity in patients recovering from acute optic neuritis. Neurolmage, 2008, 42, 836-844.	2.1	14
56	Optimizing the electric field strength in multiple targets for multichannel transcranial electric stimulation. Journal of Neural Engineering, 2021, 18, 014001.	1.8	14
57	Amygdala signals subjective appetitiveness and aversiveness of mixed gambles. Cortex, 2015, 66, 81-90.	1.1	13
58	Infinite von Mises–Fisher Mixture Modeling of Whole Brain fMRI Data. Neural Computation, 2017, 29, 2712-2741.	1.3	13
59	Risk for affective disorders is associated with greater prefrontal gray matter volumes: A prospective longitudinal study. NeuroImage: Clinical, 2018, 17, 786-793.	1.4	13
60	Predictive assessment of models for dynamic functional connectivity. Neurolmage, 2018, 171, 116-134.	2.1	13
61	Unmixing Oscillatory Brain Activity by EEG Source Localization and Empirical Mode Decomposition. Computational Intelligence and Neuroscience, 2019, 2019, 1-15.	1.1	13
62	Monocular Visual Deprivation Suppresses Excitability in Adult Human Visual Cortex. Cerebral Cortex, 2011, 21, 2876-2882.	1.6	12
63	Chasing probabilities — Signaling negative and positive prediction errors across domains. NeuroImage, 2016, 134, 180-191.	2.1	12
64	Classification of social anhedonia using temporal and spatial network features from a social cognition fMRI task. Human Brain Mapping, 2019, 40, 4965-4981.	1.9	12
65	Limited Colocalization of Microbleeds and Microstructural Changes after Severe Traumatic Brain Injury. Journal of Neurotrauma, 2020, 37, 581-592.	1.7	12
66	A Bayesian reanalysis of the effects of hydroxychloroquine and azithromycin on viral carriage in patients with COVID-19. PLoS ONE, 2021, 16, e0245048.	1.1	12
67	fMRI neuroinformatics. IEEE Engineering in Medicine and Biology Magazine, 2006, 25, 112-119.	1.1	11
68	Bayesian Model Comparison in Nonlinear BOLD fMRI Hemodynamics. Neural Computation, 2008, 20, 738-755.	1.3	10
69	A schizophrenia rat model induced by early postnatal phencyclidine treatment and characterized by Magnetic Resonance Imaging. Behavioural Brain Research, 2013, 250, 1-8.	1.2	10
70	Task-Modulated Cortical Representations of Natural Sound Source Categories. Cerebral Cortex, 2018, 28, 295-306.	1.6	10
71	Migraine with aura in women is not associated with structural thalamic abnormalities. NeuroImage: Clinical, 2020, 28, 102361.	1.4	10

52 Shifted Independent Component Analysis. , 2007, , 89-96.

#	Article	IF	CITATIONS
73	Tracking of rigid head motion during <scp>MRI</scp> using anÂ <scp>EEG</scp> system. Magnetic Resonance in Medicine, 2022, 88, 986-1001.	1.9	10
74	Identifying Schizo-Obsessive Comorbidity by Tract-Based Spatial Statistics and Probabilistic Tractography. Schizophrenia Bulletin, 2020, 46, 442-453.	2.3	9
75	Functional neuroimaging of recovery from motor conversion disorder: A case report. NeuroImage, 2019, 190, 269-274.	2.1	9
76	Associations of neural processing of reward with posttraumatic stress disorder and secondary psychotic symptoms in trauma-affected refugees. Högre Utbildning, 2020, 11, 1730091.	1.4	9
77	Modeling latency and shape changes in trial based neuroimaging data. , 2011, , .		8
78	Recovery from an acute relapse is associated with changes in motor resting-state connectivity in multiple sclerosis. Journal of Neurology, Neurosurgery and Psychiatry, 2016, 87, 912-914.	0.9	8
79	Linking brain activity during sequential gambling to impulse control in Parkinson's disease. NeuroImage: Clinical, 2020, 27, 102330.	1.4	8
80	Functional and Structural Plasticity Co-express in a Left Premotor Region During Early Bimanual Skill Learning. Frontiers in Human Neuroscience, 2020, 14, 310.	1.0	8
81	Novel Invisible Spectral Flicker Induces 40 Hz Neural Entrainment with Similar Spatial Distribution as 40 Hz Stroboscopic Light. Journal of Alzheimer's Disease, 2022, 88, 335-344.	1.2	8
82	Identifying modular relations in complex brain networks. , 2012, , .		7
83	Diagnostic Approach to Functional Recovery: Functional Magnetic Resonance Imaging after Stroke. Frontiers of Neurology and Neuroscience, 2013, 32, 9-25.	3.0	7
84	The Functional Segregation and Integration Model: Mixture Model Representations of Consistent and Variable Group-Level Connectivity in fMRI. Neural Computation, 2016, 28, 2250-2290.	1.3	7
85	Cerebellar and premotor activity during a non-fatiguing grip task reflects motor fatigue in relapsing-remitting multiple sclerosis. PLoS ONE, 2018, 13, e0201162.	1.1	7
86	Unaffected twins discordant for affective disorders show changes in anterior callosal white matter microstructure. Acta Psychiatrica Scandinavica, 2016, 134, 441-451.	2.2	6
87	Alterations in the brain's connectome during recovery from severe traumatic brain injury: protocol for a longitudinal prospective study. BMJ Open, 2017, 7, e016286.	0.8	6
88	Searchlight classification based on Amplitude of Low Frequency Fluctuation and functional connectivity in individuals with obsessive-compulsive symptoms. Cognitive Neuropsychiatry, 2019, 24, 322-334.	0.7	6
89	Discrete finger sequences are widely represented in human striatum. Scientific Reports, 2020, 10, 13189.	1.6	6

90 Ergodicity-Breaking Reveals Time Optimal Economic Behavior in Humans. , 2019, , .

5

KRISTOFFER HOUGAARD

#	Article	IF	CITATIONS
91	Unsupervised segmentation of task activated regions in fMRI. , 2015, , .		4
92	Whole brain functional connectivity predicted by indirect structural connections. , 2017, , .		4
93	VARIATIONAL BAYESIAN PARTIALLY OBSERVED NON-NEGATIVE TENSOR FACTORIZATION. , 2018, , .		4
94	Processing of Positive Visual Stimuli Before and After Symptoms Provocation in Posttraumatic Stress Disorder – A Functional Magnetic Resonance Imaging Study of Trauma-Affected Male Refugees. Chronic Stress, 2020, 4, 247054702091762.	1.7	4
95	Probing Context-Dependent Modulations of Ipsilateral Premotor-Motor Connectivity in Relapsing-Remitting Multiple Sclerosis. Frontiers in Neurology, 2020, 11, 193.	1.1	4
96	Ergodicity-breaking reveals time optimal decision making in humans. PLoS Computational Biology, 2021, 17, e1009217.	1.5	4
97	Functional magnetic resonance imaging corresponds to Humphrey perimetry in a patient with pituitary adenoma. Acta Ophthalmologica, 2005, 84, 267-268.	0.4	3
98	Task relevance differentially shapes ventral visual stream sensitivity to visible and invisible faces. Neuroscience of Consciousness, 2016, 2016, niw021.	1.4	3
99	Independent vector analysis for capturing common components in fMRI group analysis. , 2016, , .		3
100	The effect of effort-reward imbalance on brain structure and resting-state functional connectivity in in individuals with high levels of schizotypal traits. Cognitive Neuropsychiatry, 2021, 26, 166-182.	0.7	3
101	Uncovering the genetic profiles underlying the intrinsic organization of the human cerebellum. Molecular Psychiatry, 2022, 27, 2619-2634.	4.1	3
102	Identification of non-linear models of neural activity in BOLD fMRI. , 0, , .		2
103	Whole-Brain Exploratory Analysis of Functional Task Response Following Erythropoietin Treatment in Mood Disorders: A Supervised Machine Learning Approach. Frontiers in Neuroscience, 2019, 13, 1246.	1.4	2
104	The probabilistic tensor decomposition toolbox. Machine Learning: Science and Technology, 2020, 1, 025011.	2.4	2
105	Reward signalling in brainstem nuclei under fluctuating blood glucose. PLoS ONE, 2021, 16, e0243899.	1.1	2
106	Data-driven separation of MRI signal components for tissue characterization. Journal of Magnetic Resonance, 2021, 333, 107103.	1.2	2
107	Scalable group level probabilistic sparse factor analysis. , 2017, , .		1
108	Evaluating Models of Dynamic Functional Connectivity Using Predictive Classification Accuracy. , 2018, , .		1

#	Article	IF	CITATIONS
109	Dopamine agonist treatment increases sensitivity to gamble outcomes in the hippocampus in de novo Parkinson's disease. NeuroImage: Clinical, 2020, 28, 102362.	1.4	1
110	Skull segmentation from MR scans using a higher-order shape model based on convolutional restricted Boltzmann machines. , 2018, , .		1
111	Frequency constrained ShiftCP modeling of neuroimaging data. , 2011, , .		0
112	Variational group-PCA for intrinsic dimensionality determination in fMRI data. , 2016, , .		0
113	Adaptive smoothing in fMRI data processing neural networks. , 2017, , .		0
114	Modeling dynamic functional connectivity using a wishart mixture model. , 2017, , .		0
115	Testing group differences in state transition structure of dynamic functional connectivity models. , 2018, , .		0
116	Two Coarse Spatial Patterns of Altered Brain Microstructure Predict Post-traumatic Amnesia in the Subacute Stage of Severe Traumatic Brain Injury. Frontiers in Neurology, 2020, 11, 800.	1.1	0
117	Decoding Complex Cognitive States Online by Manifold Regularization in Real-Time fMRI. Lecture Notes in Computer Science, 2012, , 76-83.	1.0	0
118	Mapping cortico-subcortical sensitivity to 4 Hz amplitude modulation depth in human auditory system with functional MRI. NeuroImage, 2021, , 118745.	2.1	0
119	Uncovering Cortical Units of Processing From Multi-Layered Connectomes. Frontiers in	1.4	О